Fgf10 expression identifies parabronchial smooth muscle cell progenitors and is required for their entry into the smooth muscle cell lineage

Arnaud A. Mailleux[1,*], Robert Kelly[2], Jacqueline M. Veltmaat[†], Stijn P. De Langhe[3,†], Stephane Zaffran[2], Jean Paul Thiery[1] and Saverio Bellusci[1,†,‡]

[1]UMR144-CNRS/Institut Curie, 75248 Paris cedex 05, France
[2]URA 2578 CNRS, Department of Developmental Biology, Institut Pasteur, 25 rue du Dr Roux, 75015 Paris, France
[3]Department for Molecular Biomedical Research, Flanders Interuniversity Institute for Biotechnology (VIB)-Ghent University, Technologiepark 927, B-9052 Ghent, Zwijnaarde, Belgium

*Present address: Department of Cell Biology, Harvard Medical School, 240 Longwood Avenue, Boston, MA 02115, USA
†Present address: Developmental Biology Program, Saban Research Institute of Childrens Hospital Los Angeles, Los Angeles, CA 90027, USA
‡Author for correspondence (e-mail: sbellusci@chla.usc.edu)

Accepted 27 February 2005

Development 132, 2157-2166
Published by The Company of Biologists 2005
doi:10.1242/dev.01795

Summary

Lineage formation in the lung mesenchyme is poorly understood. Using a transgenic mouse line expressing *LacZ* under the control of *Fgf10* regulatory sequences, we show that the pool of *Fgf10*-positive cells in the distal lung mesenchyme contains progenitors of the parabronchial smooth muscle cells. *Fgf10* gene expression is slightly repressed in this transgenic line. This allowed us to create a hypomorphic *Fgf10* phenotype by expressing the *LacZ* transgene in a heterozygous *Fgf10* background. Hypomorphic *Fgf10* mutant lungs display a decrease in β-galactosidase-positive cells around the bronchial epithelium associated with an accumulation of β-galactosidase-expressing cells in the distal mesenchyme. This correlates with a marked reduction of α smooth muscle actin expression, thereby demonstrating that FGF10 is mostly required for the entry of mesenchymal cells into the parabronchial smooth muscle cell lineage. The failure of exogenous FGF10 to phosphorylate its known downstream targets ERK and AKT in lung mesenchymal cultures strongly suggests that FGF10 acts indirectly on the progenitor population via an epithelial intermediate. We provide support for a role of epithelial BMP4 in mediating the formation of parabronchial smooth muscle cells.

Key words: *Fgf10*, *Bmp4*, Smooth muscle cells, Lung, Progenitors, Differentiation, Epithelial-mesenchymal interaction, Mouse

Introduction

Despite the wealth of knowledge about the origin and differentiation of lung epithelial cells, extremely little is known about the origin and differentiation of the various lung mesenchymal cell types, i.e. the parabronchial and alveolar smooth muscle cells (SMCs), the endothelial cells, the pericytes, lipocytes and stromal fibroblasts. Yet, insight into the origin and generation of these cell types is extremely important, as they are crucial for normal respiratory function. This is illustrated by an overproliferation of bronchial SMCs associated with asthma (reviewed by Lazaar, 2002) and broncho-pulmonary dysplasia (reviewed by Hershenson et al., 1997). In addition, overproliferation of lung fibroblasts causes the respiratory problems associated with lung fibrosis (Raghu et al., 1998).

Given the significance of the distal lung tips for the establishment of lung epithelial lineages (reviewed by Warburton et al., 2000), we considered the possibility that the distal tips have a similar significance for the lung mesenchymal lineages. We focused in particular on a putative role for fibroblast growth factor 10 (FGF10) in this process, as it is specifically expressed in the distal lung mesenchyme (Bellusci et al., 1997b). Homozygous null mutants for *Fgf10* display complete lung agenesis (Min et al., 1998; Sekine et al., 1999), and can therefore not be used to study the role of *Fgf10* in the establishment of lung mesenchymal lineages. Instead, we took advantage of the recently reported *Mlcv1v-nLacZ-24* transgenic mouse strain (Kelly et al., 2001). In this strain the transgene was inserted 120 kb upstream of the *Fgf10* gene, and due to positional effects, *LacZ* expression appeared to be a true reporter for *Fgf10* expression in the developing heart (Kelly et al., 2001). Given that tissue-specific enhancer sequences drive tissue-specific gene expression, it remains to be determined whether this mouse strain is also a useful reporter for *Fgf10* expression in other organs, in this case the lung.

Here, we first demonstrate that *LacZ* expression in *Mlc1v-nLacZ-24* mice faithfully mimicked *Fgf10* expression in the developing lung, and excluded a contribution of the *Mlc1v* promoter sequences to *LacZ* expression. Analyzing the expression profile of *Mlc1v-nLacZ-24* (hereafter named $Fgf10^{LacZ}$ for simplicity), we show that *Fgf10*-positive cells in the distal mesenchyme were progenitors for the parabronchial

SMCs. Next, we demonstrate that the integration of the transgenic cassette resulted in decreased expression from the *Fgf10* gene. We obtained *Fgf10* hypomorphic mutants, by generating heterozygous *Fgf10* embryos that were hemizygous for transgenic insertion: *Fgf10*$^{+/-}$;*Mlc1v-nLacZ-24*$^{+/-}$ (hereafter called *Fgf10*$^{LacZ/-}$). In *Fgf10*$^{LacZ/-}$ lungs, part of the β-galactosidase/*Fgf10*-positive cells failed to leave the distal tip mesenchyme to become SMCs. Therefore, we postulate that *Fgf10*-positive cells in the distal lung mesenchyme are progenitors for parabronchial SMCs and, moreover, that *Fgf10* is required for their entry into the smooth muscle cell lineage.

Materials and methods

In-situ hybridization and X-gal staining

Whole-mount in-situ hybridization protocols were based on previously described methods (Winnier et al., 1995). The following mouse cDNAs were used as templates for the synthesis of digoxigenin-labeled riboprobes: a 2 kb full-length *nLacZ* cDNA (Kelly et al., 2001); a 584 bp *Fgf10* cDNA (Bellusci et al., 1997b); a 948 bp full-length mouse *Spry2* cDNA (Mailleux et al., 2004); a 642 bp *Shh* cDNA (Bellusci et al., 1997a); a 1.5 kb full-length mouse *Bmp4* cDNA; and a 90 bp *Mlc1v* cDNA (Lyons et al., 1990). To determine relative expression levels in mutants compared with wild-type embryos, they were all processed in the same tube. *LacZ* expression on whole-mount lungs was monitored by detecting β-galactosidase activity as described by Kelly et al. (Kelly et al., 1995). Sections were subsequently cut at 35 μm with a vibratome or at 5 μm with a microtome after paraffin embedding.

Mutant embryos

The *Mlc1v-nLacZ-24* line is bred in a mixed background and has been previously described (Kelly et al., 2001). The transgene containing an *nLacZ* reporter gene is integrated upstream of the *Fgf10* gene. *Fgf10*$^{LacZ/-}$ mouse embryos were generated by crossing *Fgf10*$^{+/-}$ on a C57Bl/6 background (Sekine et al., 1999) with *Mlc1v-nLacZ-24*$^{+/-}$ mice (Kelly et al., 2001). Wild-type littermates were used as control embryos at different developmental stages. The *Fgf10*$^{-}$ and *Mlc1v-nLacZ-24*$^{+}$ alleles were genotyped as described previously (Mailleux et al., 2002; Kelly et al., 2001). The number of *Fgf10*$^{LacZ/-}$ embryos used in this study (52 in total) at the different stages was as follows: embryonic day (E) 12.5 (n=7); E13.5 (n=3); E14.5 (n=6); E16.5 (n=2); E17.5 (n=10); E18.5 (n=7); P_0 (n=17). For simplicity, the *Mlc1v-nLacZ-24*$^{+/-}$ is called *Fgf10*$^{LacZ/+}$; the *Mlc1v-nLacZ-24*$^{+/+}$ is called *Fgf10*$^{LacZ/LacZ}$; *the Fgf10*$^{+/+}$;*Mlc1v-nLacZ-24*$^{+/-}$ is called *Fgf10*$^{LacZ/+}$ while the *Fgf10*$^{+/-}$;*Mlc1v-nLacZ-24*$^{+/-}$ is called *Fgf10*$^{LacZ/-}$. The *SpC-Bmp4* (n=3 at E16.5) and *SpC-Shh* (n=4 at E16.5) transgenic embryos have been generated previously (Bellusci et al., 1996; Bellusci et al., 1997a).

Whole-lung culture, cyclopamine treatment and distal mesenchyme grafting

Embryonic lungs were removed at E11.5 and placed on Nuclepore Filters (8 μm pore diameter) in 30 μl of a 1:1 mixture of Matrigel and culture medium (DMEM/F12 medium containing penicillin/streptomycin and 0.1% heat-inactivated fetal bovine serum). After 30 minutes at 37°C to allow the Matrigel to polymerize, these filters were laid on the surface of 500 μl culture medium containing cyclopamine (TRC Biomedical Research Chemicals, Canada) in Nunclon dishes (technique adapted from Lebeche et al., 1999). Concentrations of 1, 2, 5, 10 and 15 μmol/l cyclopamine were tested as previously described (Yao et al., 2002). At 10 and 15 μmol/l, cyclopamine was toxic. Explants were cultured for 1 day in the presence of cyclopamine and then fixed in 4% PFA (15 minutes at 4°C) before X-gal staining. For distal mesenchyme grafting, the distal part (mesenchyme and mesothelium) of the accessory or median lobes of wild-type and *Fgf10*$^{LacZ/+}$ lungs at E12.5 were dissected with tungsten needles in culture medium. *Fgf10*$^{LacZ/+}$ and wild-type lungs were reciprocally grafted in 1:1 Matrigel:culture medium on Nuclepore Filters using tungsten needles. After 30 minutes polymerization of the Matrigel at 37°C, 500 μl culture medium was added under the filter. Grafts were cultured for 44 hours (37°C, 6% CO_2), fixed in 4% PFA and X-gal stained as described above.

Distal mesenchyme labeling and video-cinematography

The distal part of wild-type accessory lobe mesenchyme was dissected and incubated with the Cell Tracker Green CMFDA (Molecular Probe; 20 μmol/l in DMEM/F12 medium) for 20 minutes in the dark at room temperature. The labeling mixture was prepared following the manufacturer's instructions. The distal parts were then grafted back at the tip of the accessory lobe they were derived from. Time-lapse video-cinematography was started 18 hours post-grafting using a LEICA inverted microscope equipped with a temperature and CO_2 controlled chamber and a Princeton Micromax CDD camera as described previously (Murase and Horwitz, 2002). The experiments have been carried out over a 24-48 hour period. With this in-vitro system, the position of the most external edges of the lung mesenchyme did not significantly change and was used as the reference point in order to follow the putative migration of the mesenchymal cells within this time frame.

Semi-quantitative RT-PCR

Total RNA was extracted from a pool of three lungs at E14.5 per genotype using the RNeasy Total RNA kit (Qiagen). The RNA was reverse-transcribed using hexamers with TaqMan Transcript Reagent kit (Applied Biosystem) according to the manufacturer's conditions. One-fiftieth of the cDNA prepared from 1 μg RNA was subjected to PCR using murine gene-specific primers for *Fgf10* (5′-TGTTTTTTTGTCCTCTCCTGGGAG-3′ and 5′-GGATACTGACA-CATTGTGCCTCAG-3′), *Bmp4* (5′-GAACAGGGCTTCCACCGTA-3′ and 5′-TGAGGTGTCCAGGAACCAT-3′), *Spry2* (5′-CTC-CACTCAGCACAAACAT-3′ and 5′-TTGTCCTTGTATGCTCCGA-3′) and tubulin (5′-TGGCCAGATCTTCAGACCAG-3′ and 5′-GTA-AGTTCAGGCACAGTGAG-3′) as internal control. No amplicons were detected in water and minus RT control. For semiquantitative PCR, target sequences were amplified within the linear amplification range between 25 and 34 cycles at 55°C in order to yield visible products. PCR products were separated by electrophoresis on a 1.5% agarose gel and stained with ethidium bromide. Photographs were taken with a Vilbert-Loumart apparatus and the intensity of the bands was determined by densitometry with NIH Image software (http://rsb.info.nih.gov/nih-image/) using Gel Plotting Macros (ftp://rsbweb.hih.gov/pub/nih-image/macros/). Expression of *Fgf10*, *Bmp4* and *Spry2* were determined relative to tubulin expression.

Cultures of isolated lung mesenchyme explants

Explants consisted of the total mesenchyme distal to the primary bronchi of wild-type and *Flk1*$^{LacZ/+}$ (Shalaby et al., 1995) E11.5 lungs. They were cultured in Matrigel™ (Bellusci et al., 1997b) for 48 hours in the presence of 0, 50, 100 and 150 ng/ml BMP4 (R&D). BMP4 (100 ng/ml) was the optimal dose to induce α-SMA expression in the mesenchyme, and this dose was used throughout the study (n=4). The explants were then fixed in PFA 4%, dehydrated, embedded in paraffin and sectioned at 7 μm. *Flk1*$^{LacZ/+}$ explants were stained with X-gal before embedding.

Preparation of mesenchymal cell cultures and FGF treatment

Whole lungs were dissected at E13.5 and subjected to trypsin digestion to give rise to single cells. Mesenchymal cells were separated from epithelial cells by differential adhesion as described

previously (Lebeche et al., 1999; Yang et al., 1999). Mesenchymal cells were cultured for 4 hours (undifferentiated cells) or 48 hours (differentiated cells) in DMEM/F12 medium containing penicillin/streptomycin and 0.5% heat-inactivated fetal bovine serum for starvation. They were subsequently cultured during 20 minutes with 100 ng/ml of recombinant FGF1, FGF7 and FGF10, respectively (R&D Systems). Protein extracts and immunoblot analysis were performed as described previously (Yang et al., 1999).

Antibodies

A Cy3-conjugated mouse monoclonal antibody against α-SMA, (Sigma, C-6198), pan-Cytokeratine (Dako), β-galactosidase (US Biological, G1041-42) were used at a dilution of 1/200 for immunohistochemistry. For immunoblot analysis, rabbit polyclonal antibodies against phospho-AKT (Ser473, #9271), AKT (#9272), phospho-p44/42 MAP kinase (#9101) and p44/42 MAP kinase (#9102) were obtained from Cell Signalling Technology, and used according to the manufacturer's instructions.

Results

Expression of the *Mlc1v-nLacZ-24* transgene in the developing lung faithfully represents expression of the *Fgf10* gene

We first analyzed whether *Mlc1v-nLacZ-24* transgenic expression represents expression from the *Fgf10* locus in the developing lung, similar to previous observations in the heart (Kelly et al., 2001). By whole-mount in-situ hybridization we could not detect any endogenous *Mlc1v* mRNA in the lung at E12.5 and 13.5, whereas we did detect *Mlc1v* mRNA expression in the internal control tissue: the cardiac muscle (data not shown). This strongly suggested that the endogenous *Mlc1v* gene promoter is inactive in the developing lung, and that it may therefore be concluded that the *Mlc1v* promoter sequences in the transgenic cassette do not drive *LacZ* expression in the lung. To further support this, we used a model of in-vitro smooth muscle cell differentiation in primary cultures of embryonic lung mesenchymal cells (Yang et al., 1998). If the myosin light chain ventricular 1 promoter of the transgene drives a residual expression in the smooth muscle cells of the *Mlc1v-nLacZ-24*$^{+/-}$ lungs, we would expect 100% of the cells to be simultaneously positive for β-galactosidase and alpha smooth muscle actin (α-SMA). Indeed, all the mesenchymal cells expressed α-SMA after 44 hours of culture. However, only a fraction of these cells were β-galactosidase-positive (data not shown), suggesting that the *Mlc1v* promoter is indeed inactive in the *Mlc1v-nLacZ-24*$^{+/-}$ line.

We next compared the expression pattern of the transgene in lungs of *Mlc1v-nLacZ-24* hemizygous embryos to *Fgf10* expression in wild type lungs, at the level of either *LacZ* mRNA expression or β-galactosidase activity. At E10.5, the distal tip of the right lobe (black arrow), but not the left lobe, expressed *Fgf10* mRNA (Fig. 1A). One day later, the right lobe had subdivided into four lobes. Each of these lobes expressed *Fgf10* mRNA at the distal tips (Fig. 1C). At this time, the left lobe had also started to express *Fgf10* mRNA (dashed boxed area in Fig. 1C). We have previously shown that the distal *Fgf10* expression is exclusively mesenchymal (Bellusci et al., 1997b). We detected β-galactosidase activity in a very similar pattern at E10.5 (Fig. 1B) and E11.5 (Fig. 1D). The absence of β-galactosidase activity in the left lobe at E11.5 (boxed area in Fig. 1D) may reflect the delayed onset of expression of *Fgf10* in the left lobe, as already observed at E10.5. Analysis of *LacZ* expression as mRNA (Fig. 1G,H) or as β-galactosidase activity (Fig. 1I,J) at E12.5 revealed that its expression was still highly similar to the expression pattern of *Fgf10* mRNA at the mesenchymal edges of each lobe adjacent to the distal ends of the bronchi (Fig. 1E,F) (Mailleux et al., 2001). However, at this stage (Fig. 1I,J) and later at E14.5, β-galactosidase activity was additionally observed at the level of the secondary bronchi (arrow in Fig. 1L) by contrast to *Fgf10* mRNA expression (Fig. 1K). This expression corresponds to the mesenchyme adjacent to the bronchial epithelium (Fig. 2E,F). Importantly, *LacZ* expression was essentially not found in the mesenchyme of the primary bronchi except for the very distal part (black arrowhead in Fig. 1I and white arrowhead in Fig. 1L).

The difference between *LacZ* expression at the mRNA and protein level is most probably due to a higher stability of the β-galactosidase protein compared with *LacZ* mRNA, as previously observed during heart development (Kelly et al., 2001). It may indicate that cells, expressing *Fgf10* mRNA while located in the distal mesenchyme, or their daughter cells, populate the more proximal areas. In conclusion, the similarity of expression patterns of *Fgf10*, *LacZ* and β-galactosidase activity, combined with the lack of detection of *Mlc1v* transcripts in the developing lung, strongly suggests that expression of the *Mlc1v-nLacZ-24* transgene is exclusively driven by *Fgf10* regulatory sequences and completely and solely represents the *Fgf10* expression pattern in the developing lung.

To further validate the use of the *Mlc1v-nLacZ-24* transgene as a reporter for *Fgf10* expression, we analyzed the control of *LacZ* expression by *Fgf10* regulatory elements in a functional assay. We made use of the knowledge that sonic hedgehog (SHH) downregulates *Fgf10* expression in the lung (Bellusci et al., 1997b; Pepicelli et al., 1998; Lebeche et al., 1999), and that cyclopamine is a specific inhibitor of SHH function (Yao et al., 2002). Lungs derived from E11.5 hemizygous *Mlc1v-nLacZ-24* embryos, and cultured for 28 hours in the presence of 5 μmol/l cyclopamine displayed dilated epithelium (arrows in Fig. 1S,O). A similar phenotype was previously observed upon addition of recombinant FGF10 on lung grown in vitro (Bellusci et al., 1997b), suggesting that cyclopamine treatment triggers *Fgf10* upregulation. An increase in β-galactosidase activity was observed compared with the untreated lung (compare Fig. 1P-U). The effect of cyclopamine upon β-galactosidase activity was particularly apparent in the left lobe (arrows in Fig. 1P,T). These observations support our expression data and indicate that *LacZ* expression in the *Mlc1v-nLacZ-24* strain can be used as a reporter for *Fgf10* expression. In accordance with this conclusion, we will hereafter refer to the mice heterozygous for the *Mlc1v-nLacZ-24* cassette as *Fgf10*$^{LacZ/+}$ mice.

Fgf10-positive cells in the distal mesenchyme give rise to parabronchial smooth muscle cells

The β-galactosidase expression domain expanded progressively from the peripheral distal mesenchyme toward the distal epithelium between E11.5 and 12.5 (Fig. 2A-D), whereas the *Fgf10* and *LacZ* mRNAs remained expressed only in the peripheral mesenchyme at this time (Fig. 1D and double pointed arrows in Fig. 1F,H). This supports the presumption that cells from the peripheral distal mesenchyme or their daughter cells

can relocate to more proximal areas. Vibratome sections of the accessory lobe at E12.5 illustrate that the β-galactosidase-positive cells were exclusively located in the mesenchyme throughout the distal tip mesenchyme and as one layer adjacent to the proximal epithelium (Fig. 2E). Transversal sections in the most proximal part of E12.5$^{LacZ/+}$ accessory lobe show that β-galactosidase expression entirely surrounded the epithelium of the secondary bronchi (Fig. 2E'). In addition, at this stage not all the mesenchymal cells directly adjacent to the epithelium were positive for β-galactosidase (Fig. 2E, red arrows), in harmony with the patchy β-galactosidase expression pattern in whole-mount staining of the accessory lobe (arrow in Fig. 2D). By E13.5, the β-galactosidase-positive cells had formed a continuous layer adjacent to the epithelium (Fig. 2F).

The location of these cells suggested that they could be parabronchial SMCs. Indeed, they co-expressed the smooth muscle cell marker α-SMA around the bronchial epithelium (Fig. 2G). Fig. 2H,I show additionally that α-SMA was not expressed in the distal tip mesenchyme, but was restricted to the layer of mesenchymal cells directly in contact with the proximal bronchial epithelium.

In conclusion, the dynamics of the β-galactosidase expression pattern strongly suggests that the mesenchymal *Fgf10*/β-galactosidase-positive cells in the distal tip represent smooth muscle cell progenitors.

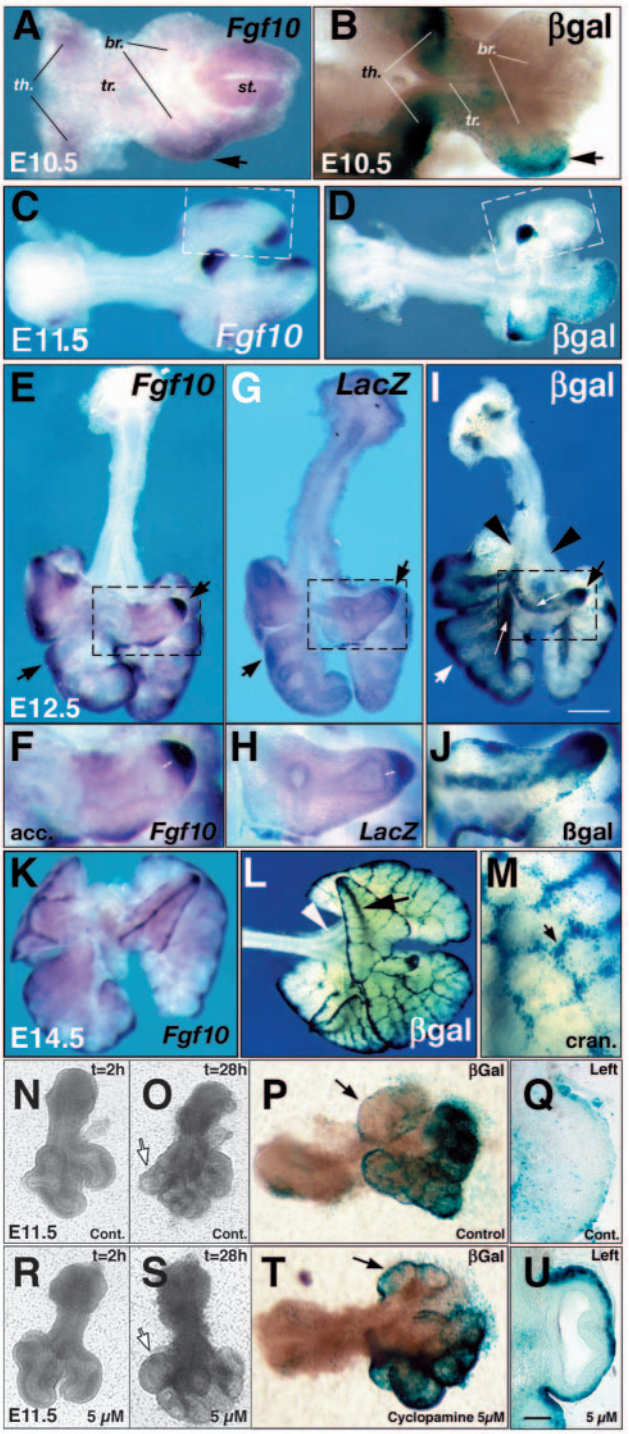

Fig. 1. *Mlc1v-nLacZ-24*$^{+/-}$ expression recapitulates *Fgf10* expression. (A) *Fgf10* expression by whole-mount in-situ hybridization in E10.5 wild-type control lungs. Note the expression in the right distal lung mesenchyme (black arrows), the thyroid and the developing stomach. (B) X-gal-stained E10.5 *Mlc1v-nLacZ-24*$^{+/-}$ lungs recapitulate the *Fgf10* expression pattern at this stage in the distal lung mesenchyme (black arrow) and the thyroid. (C) *Fgf10* expression by whole-mount in-situ hybridization in E11.5 wild-type control lungs. Note the expression in the left distal lung mesenchyme (white dotted box). (D) X-gal staining of E11.5 *Mlc1v-nLacZ-24*$^{+/-}$ lungs recapitulates the *Fgf10* expression pattern at this stage, except in the left lobe (white dotted box). (E) *Fgf10* expression by whole-mount in-situ hybridization in E12.5 wild-type control lungs. Note the expression in the distal lung mesenchyme (black arrows). The area in the dotted box is magnified in (F). (G) *LacZ* expression at RNA level in *Mlc1v-nLacZ-24*$^{+/-}$ lungs. (H) *LacZ* is expressed at the tip of the accessory lobe recapitulating the *Fgf10* pattern (dotted box in G). Notice the absence of *Fgf10* expression close to the epithelium (small double white arrow) (I) β-galactosidase activity shown by X-gal staining is found in the distal mesenchyme (white arrow) and at the level of the bronchi of *Mlc1v-nLacZ-24*$^{+/-}$ lungs (small white arrows). Note that X-gal staining is now present in the mesenchyme of the left lobe. Note also that β-galactosidase-positive cells are not detected in the primary bronchi (black arrows). (J) High magnification of the accessory lobe (dotted box in I). (K) *Fgf10* expression at RNA level by whole-mount in-situ hybridization in E14.5 wild-type control lungs. Note the expression in the mesenchyme at the periphery of the lobes. (L) X-gal staining of E14.5 *Mlc1v-nLacZ-24*$^{+/-}$ lungs showing *LacZ* expression at the periphery of the lobes similar to the *Fgf10* expression pattern. Note β-gal expression at the level of the bronchi (black arrow). (M) High magnification of the surface of the cranial lobe shown in L. (N-Q) Control E11.5 *Mlc1v-nLacZ-24*$^{+/-}$ lung grown in absence of cyclopamine. (O) After 28 hours in culture new branches are formed. Note that the distal epithelium is not dilated (arrow). (P) X-gal staining of the cultured lung shown in O. β-gal expression is found in the distal mesenchyme. (Q) Vibratome section through the left lobe shown by the arrow in P. Note the low level of β-gal expression. (R-U) E11.5 *Mlc1v-nLacZ-24*$^{+/-}$ lung grown in presence of 5 μmol/l of cyclopamine. (S) After 28 hours of culture the lung exhibits dilated end buds (arrow). (T) X-gal staining of the cultured lung shown in S. Note the increase in β-gal expression throughout the lung in comparison with the lung grown in the absence of cyclopamine shown in P. (U) Vibratome section through the left lobe of the lung shown by the arrow in T. Note the marked increase in *LacZ* expression compared with the untreated lung (Q). Scale bar: 110 μm in A,B; 180 μm in C,D; 210 μm in E,G,I; 105 μm in F,H,J; 435 μm in K,L; 80 μm in M; 175 μm in J; 250 μm in N,O; 300 μm in O,S; 190 μm in P,T; 50 μm in Q,U. acc, accessory lobe; br, bronchus; cont, control; cran, cranial lobe; st, stomach; th, thyroid; tr, trachea.

Fgf10-positive mesenchymal cells passively relocate around the bronchial epithelium

In order to assess whether these proximal β-galactosidase-positive cells are indeed derived from the distal mesenchyme, we carried out reciprocal heterotypic grafts of pulmonary distal mesenchyme on lungs of wild-type and $Fgf10^{LacZ/+}$ embryos. The grafted lungs were cultured for 2 days and compared to unmanipulated $Fgf10^{LacZ/+}$ cultured lungs. In the unmanipulated lungs, the β-galactosidase-positive cells were located in the distal tip as well as in a single layer of cells around the more proximal epithelium (Fig. 3A-D).

An identical patterning of β-galactosidase-positive cells was observed in cultures of wild-type lungs grafted with $Fgf10^{LacZ/+}$ distal lung mesenchyme (Fig. 3E-H). By contrast, in cultures of $Fgf10^{LacZ/+}$ lung grafted with wild-type mesenchyme (Fig. 3I), no or few β-galactosidase positive-cells were observed proximally (Fig. 3K,L). These results demonstrate unequivocally that the proximal mesenchymal β-galactosidase-positive cells originate from the *Fgf10*-positive distal tip mesenchyme. They additionally support our notion that the *Mlc1v* promoter sequences do not drive *LacZ* expression in the developing lung.

To assess how distal mesenchymal cells populate the more proximal areas, the distal part of a wild-type lung (mesenchyme and mesothelium) was dissected out from the accessory lobe, re-implanted after staining with the fluorescent marker CMFDA and followed up for 25 hours by video-cinematography. Our results show no relative movement of the labeled cells with respect to the epithelium and no cells leaving the labeled explant (Fig. 3M,N). This suggests that mesenchymal cells do not actively migrate along the epithelium but passively relocate during epithelial outgrowth into the distal mesenchyme.

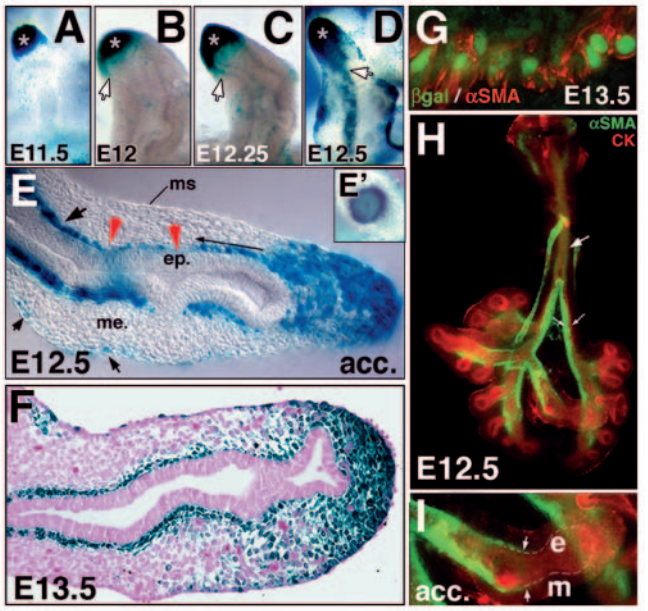

Fig. 2. *Fgf10*-positive mesenchymal cells give rise to parabronchial smooth muscle cells. (A-D) Timecourse of β-galactosidase expression in the accessory lobe between E11.5 and 12.5, showing the progressive extension of *LacZ* expression from distal mesenchyme (asterisk) toward the epithelium (arrow). Note the patchy expression of β-galactosidase around the secondary bronchi at E12.5 (D). (E) A saggital vibratome section through an E12.5 $Fgf10^{LacZ/+}$ accessory lobe showing almost continuous flow of β-galactosidase expression in the distal mesenchyme (asterisk) and around the distal and proximal epithelium (arrows). Note that not all the cells around the epithelium of the secondary bronchi are positive for β-galactosidase (red arrows). (E') A transversal section in secondary bronchus located in the most proximal part of E13.5$^{LacZ/+}$ accessory lobe show that β-galactosidase expression is found in the mesenchyme all around the epithelium. (F) Saggital section of E13.5 $Fgf10^{LacZ/+}$ accessory lobe showing a continuous layer of β-galactosidase-positive cells around the secondary bronchus. (G) Co-localization by immunofluorescence of β-galactosidase (in green; note the nuclear signal) and α-SMA (in red). (H) Whole-mount immunohistochemistry with anti-cytokeratin (in red) and anti-SMA (in green) antibodies on E12.5 lung. Note the presence of α-SMA expression around the bronchi (small white arrows) and the absence of α-SMA expression in the ventral part of the trachea (white arrow). (I) High magnification of the accessory lobe shown in H, demonstrating the absence of α-SMA expression in the most distal part of the lung. Scale bars: 210 μm in A,B; 240 μm in C; 270 μm in D; 120 μm in E,F; 450 μm in H; 200 μm in I.

Reduction of *Fgf10* expression in the lung leads to decreased smooth muscle actin expression around the bronchi

We noted that $Fgf10^{LacZ/+}$ mice, similar to *Fgf10* heterozygous mice, have smaller eyelids and a moderate nervous behavior compared with wild-type mice. We therefore tested whether the insertion of the *Mlvc1v-nLacZ* cassette 120 kb upstream of the transcriptional start site of the *Fgf10* gene reduces *Fgf10* expression. Indeed, whole-mount in-situ experiments showed decreased *Fgf10* expression in $Fgf10^{LacZ/LacZ}$ embryos when compared with wild-type littermates (Fig. 4A,B). This indicates that the insertion of the transgenic cassette creates a hypomorphic *Fgf10* allele. It furthermore suggests that an allelic series can be generated by crossing hemizygous or homozygous $Fgf10^{LacZ}$ mice with heterozygous *Fgf10* null mice.

Fifty-two $Fgf10^{LacZ/-}$ compound heterozygous embryos were obtained at Mendelian ratio between E12.5 and P0. Semi-quantitative RT-PCR was performed on RNA isolated from a pool of three lungs per genotype at E14.5 (Fig. 4C). The results indicate a gradual decrease of *Fgf10* mRNA expression in $Fgf10^{LacZ/+}$, $Fgf10^{+/-}$ and $Fgf10^{LacZ/-}$ compound heterozygous mice, confirming the generation of an allelic series of pulmonary *Fgf10* expression.

At E12.5, $Fgf10^{LacZ/-}$ embryos have a slightly smaller lung with decreased branching morphogenesis compared with wild-type or $Fgf10^{LacZ/+}$ lungs (Fig. 4D,E). In addition, α-SMA expression is decreased specifically around the epithelium of the secondary bronchi (n=2; Fig. 4F,G). The deposition of laminin, an extracellular matrix protein synthesized by the lung epithelium and involved in the differentiation of the SMC (Zhang et al., 1999), was not perturbed around the bronchial epithelium of $Fgf10^{LacZ/-}$ lungs (data not shown).

A similar decrease in α-SMA expression was observed at E13.5 (n=2, data not shown), E14.5 (n=2, data not shown) and E17.5 (n=3, Fig. 4I,K) compared with control lungs (Fig. 4H,J), as well as at E18.5 (n=3, data not shown) and after birth (n=2, data not shown). Elastin deposition by SMCs around the bronchi was also reduced in $Fgf10^{LacZ/-}$ lungs at birth (data not shown). In addition, a specific decrease in gelatinase activity

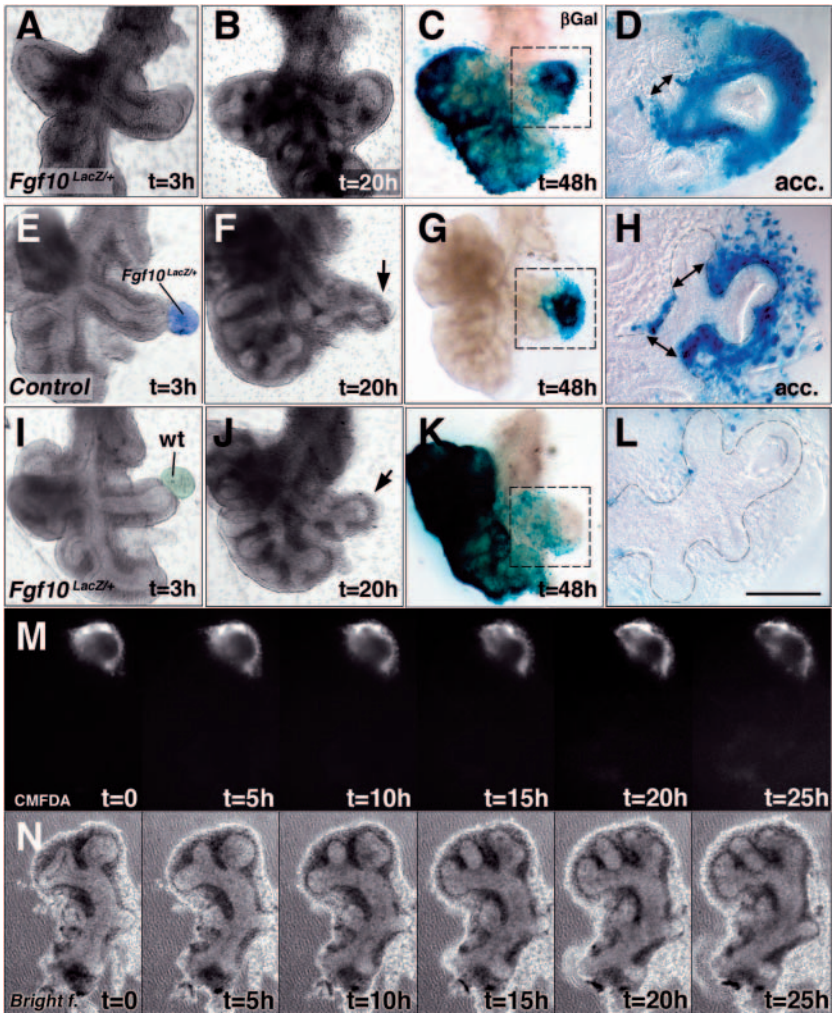

Fig. 3. *Fgf10*-positive mesenchymal cells relocate around the bronchial epithelium. (A-D) β-gal expression in the accessory lobe of unmanipulated *Fgf10*$^{LacZ/+}$ lung after 48 hours of culture. (D) Vibratome section of the accessory lobe shown in C (dotted box). Notice the presence of β-galactosidase-positive cells around the proximal epithelium (double arrow). (E-H) Grafting of *Fgf10*$^{LacZ/+}$ mesenchyme (in blue) on wild-type lungs. (H) Vibratome section of the accessory lobe shown in G (dotted box). Note the presence of β-galactosidase-positive cells around the proximal epithelium. The gray dotted line underlines the epithelium. (I-L) Ablation of the distal *Fgf10*$^{LacZ/+}$ accessory lobe mesenchyme and grafting of equivalent wild-type mesenchyme (green) results in a drastic decrease of β-gal expression around the bronchi (K,L). (L) Vibratome section of the accessory lobe shown in K (dotted box). Notice the absence of β-gal-positive cells around epithelium. The epithelium is outlined by the dotted line. (M-N) Time-lapse sequence of E12 accessory lobes after the auto-grafting of CMFDA labeled distal mesenchyme (which includes the mesothelium). (M) Twenty-five-hour time-lapse fluorescence showing that mesenchymal cells are not actively migrating along the epithelium. (N) Phase-contrast time-lapse sequence of M, showing the outgrowth and budding of the epithelium. acc, accessory lobe; Bright f, Bright Field. Scale bar: 190 μm in A,B,E,F,I,J; 165 μm in C,G,K; 45 μm in D,H,L; 60 μm in M,N.

at birth in *Fgf10*$^{LacZ/-}$ lung mesenchyme, especially in parabronchial SMCs, was revealed by in-situ zymography (data not shown). Therefore, decreased *Fgf10* expression in the distal mesenchyme clearly leads to a defect in the proper establishment of the parabronchial SMC population from early embryonic stages.

Interestingly, less β-galactosidase activity was observed around the epithelium of the secondary bronchi, while more activity was present in the distal mesenchyme of *Fgf10*$^{LacZ/-}$ lungs compared with *Fgf10*$^{LacZ/+}$ lungs (compare Fig. 4L,M). By TUNEL or PCNA analyses (data not shown), we did not see any significant changes in apoptosis or in proliferation of the parabronchial SMCs between E14.5 and 17.5.

These results suggest that FGF10 is involved directly or indirectly in the entry of the *Fgf10*/β-galactosidase-positive SMC progenitors into the SMC lineage rather than in their survival or proliferation.

FGF10 regulates SMC formation in a non-autocrine fashion, possibly via upregulation of epithelial BMP4

To test whether FGF10 acts in an autocrine fashion on the mesenchyme, or in a paracrine fashion via the epithelium, primary cultures of mesenchymal cells derived from the entire E13.5 wild-type lung were established. These were either cultured for 4 hours, sufficient for the cells to start to differentiate, or for 48 hours to lead to fully differentiated SMCs, before addition of recombinant FGF1, FGF7 or FGF10. Unlike FGF1, FGF10 and FGF7 did not upregulate ERK phosphorylation (Fig. 5A) nor AKT phosphorylation (data not shown) in undifferentiated or differentiated cultures. These results suggest that FGF10 does not act on mesenchymal cells in an autocrine fashion but via an epithelial intermediate. Previous reports have shown that *Bmp4* is a downstream epithelial target of FGF10 in the lung (Lebeche et al., 1999; Weaver et al., 2000; Mailleux et al., 2001). In harmony with these results, the expression of *Bmp4* was decreased in *Fgf10*$^{LacZ/-}$ lungs (Fig. 5C,E). The expression of *Sprouty2*, another FGF10 downstream target (Mailleux et al., 2001) was also decreased (Fig. 5D,E), while the expression of *Shh*, an upstream negative regulator of *Fgf10* expression (Bellusci et al., 1997b), was unchanged (Fig. 5B).

To test whether *Bmp4* is indeed involved in the formation of SMCs in vivo, we overexpressed it under the surfactant protein C promoter specifically in the distal lung epithelium. As a positive control, we also overexpressed *Shh* under the same promoter, as it has been shown to trigger the induction of α-SMA expression in isolated lung mesenchymal explants cultured in vitro (Weaver et al., 2003). To our surprise, *SpC-Shh* overexpression did not have an apparent effect on localization or levels of α-SMA expression in the mesenchyme (Fig. 5H), whereas *SpC-Bmp4* induced ectopic expression of α-SMA in the mesenchyme as expected (Fig. 5I). In accordance with this result, we also showed that recombinant BMP4 (100 mg/ml) directly upregulates α-SMA expression lung in mesenchyme explants (n=4) cultured in Matrigel^{TM}

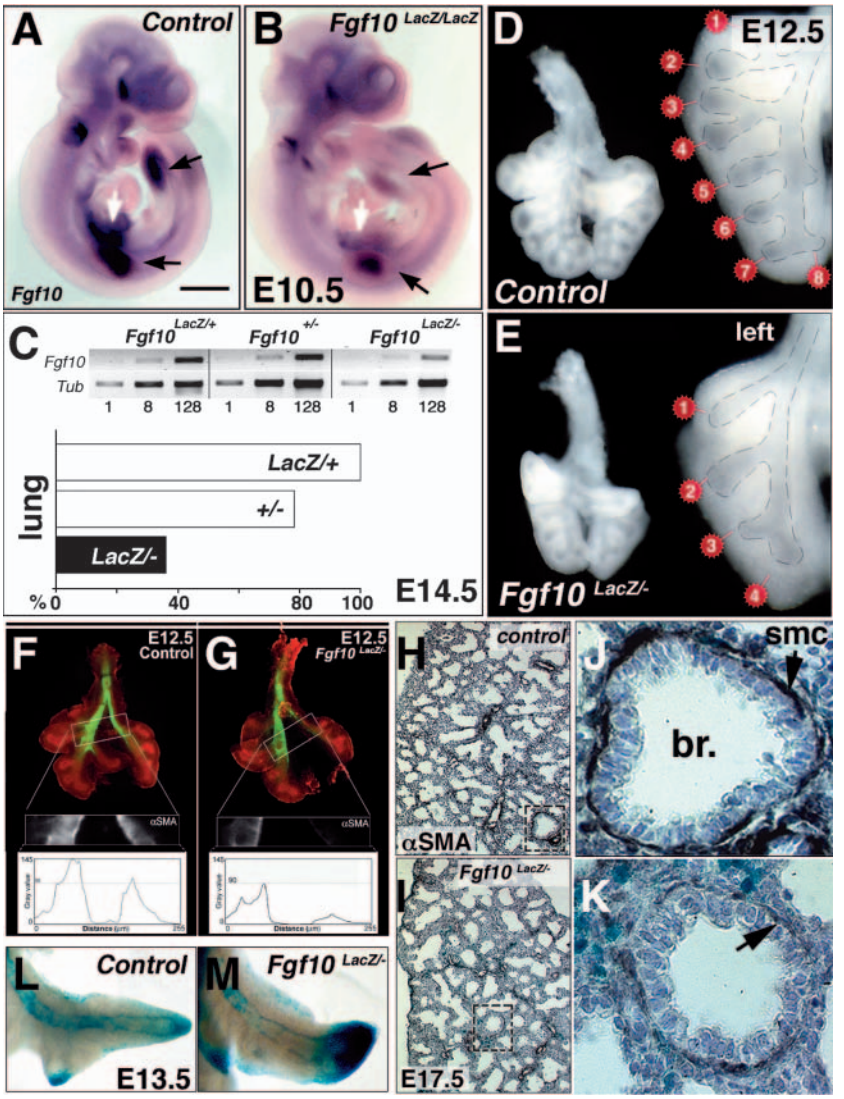

Fig. 4. Reduction of *Fgf10* expression in the lung leads to a decrease in SMA expression around the bronchi. (A-B) *Fgf10* expression shown by whole-mount in-situ hybridization in E10.5 wild-type (A) and $Fgf10^{LacZ/LacZ}$ (B) embryos. Note the reduction in *Fgf10* expression in the limbs (black arrows) and in the lung (white arrow). (C) Upper part: semi-quantitative amplification course by PCR on gel electrophoresis, respectively 1 (cycle 25), 8 (cycle 28) and 128 (cycle 32) amplification rate, showing decreased *Fgf10* mRNA level in $Fgf10^{LacZ/-}$ compared with $Fgf10^{LacZ/+}$ or $Fgf10^{+/-}$ lungs at E14.5. Lower part: quantification of *Fgf10* expression by densitometry at 128 amplification rate. Ratio of *Fgf10* expression to tubulin in $Fgf10^{LacZ/+}$ is set at 100% and used as a reference. Note the graded decrease in the expression of *Fgf10* in $Fgf10^{+/-}$ (22%) and $Fgf10^{LacZ/-}$ (64%). (D,E) Decreased lung branching in E12.5 $Fgf10^{LacZ/-}$ lungs. High magnification on the left lobe shows that E12.5 mutant lung (E) is less branched (four buds) than control lobe (eight buds) (D). The epithelium is outlined by the gray dotted line. (F-G) Whole-mount immunohistochemistry with α-SMA (in green) and cytokeratin (in red) antibodies in control (F) and $Fgf10^{LacZ/-}$ (G) lungs at E12.5. The intensity of pixels representing the expression of α-SMA around the right and left bronchi is quantified. A significant reduction (approximately 40% for the right secondary bronchi and 90% for the left secondary bronchi) is observed in the $Fgf10^{LacZ/-}$ lung. (H-K) Immunohistochemistry with α-SMA antibody on E17.5 wild-type control (H) and $Fgf10^{LacZ/-}$ lungs (I). (J) Higher magnification of the dotted box shown in H. Note the labeled smooth muscle cells around the bronchi. (K) Higher magnification of the dotted box shown in (I). Note the drastic decrease in α-SMA (white arrow) expression around the bronchi. (L) X-gal staining of E13.5 $Fgf10^{LacZ/+}$ lung, showing significant β-galactosidase signal around the epithelium of the secondary bronchi of the accessory lobe. (M) X-gal staining under the same conditions of E13.5 $Fgf10^{LacZ/-}$ lung, showing strong decrease in β-galactosidase-expressing cells around the bronchial epithelium of the secondary bronchi of the accessory lobe as well as accumulation of β-galactosidase-expressing cells at the distal tip. Scale bar: 590 μm in A,B; 150 μm in D,E right part; 300 μm in D,E left part; 150 μm F,G; 60 μm in H,I; 15 μm in J,K; 100 μm in L,M. br, bronchi; smc, smooth muscle cells.

(Fig. 5J,L). Not all the cells were positive for α-SMA after BMP4 treatment. These cells may be endothelial cells, as suggested by the presence of β-galactosidase-positive cells in mesenchymal explants from E12.5 $Flk1^{LacZ/+}$ lungs in the absence or presence of BMP4 (Fig. 5K,M). Taken together, these data strongly suggest that epithelial BMP4, a target of FGF10, controls the differentiation of cells arising from the distal mesenchymal *Fgf10*-expression domain into the parabronchial SMC lineage.

Discussion

LacZ expression in the *Mlc1v-nLacZ-24* transgenic line is a bona fide marker for *Fgf10* expression in the developing lung

By expression analysis at the RNA and protein level combined with a functional assay, we here demonstrate that expression from the *Mlc1v-nLacZ-24* transgene exclusively and completely reflects *Fgf10* expression in the murine embryonic lung. These findings are in accordance with a previous report showing that expression of this transgene reflects *Fgf10* expression in the developing heart, attributed to its integration 120 kb upstream of the *Fgf10* gene (Kelly et al., 2001). By screening the genome using the Ensembl database at http://www.ensembl.org/Mus_musculus/, we found that only one other gene was present near this integration site at the telomere of chromosome 13. It concerns the mitochondrial ribosomal protein S30 (*Mrps30*) gene, which is located 200 kb upstream of insertion of the transgenic cassette. Furthermore, unpublished work in our group has demonstrated that $Fgf10^{LacZ/-}$, embryos display a hypomorphic *Fgf10* phenotype in the gut, limb and mammary gland (S.B., unpublished). This strongly suggests that the *Mlc1v-nLacZ-24* transgene is expressed in a pattern similar to that of *Fgf10* in these organs. We therefore hypothesize that the *Mlc1v-nLacZ-24* mouse strain may be a useful reporter for *Fgf10* expression in any organ.

Fgf10 expression in the distal lung mesenchyme identifies progenitors for parabronchial SMCs

Our chimaeric lung cultures demonstrated that the distal mesenchyme gives rise to the parabronchial SMC population in more proximal areas. To date, this is the first evidence for the location of progenitors for parabronchial SMCs, as well as for their identification by the expression of *Fgf10*.

Our data indicate that β-galactosidase is essentially not present in the mesenchyme around the primary bronchi of the $Fgf10^{LacZ/+}$ lungs, while α-SMA is detected around the primary bronchi at E12.5. This difference suggests that the smooth muscle cells around the epithelium of the primary bronchi and the smooth muscle cells around the epithelium of the secondary bronchi may originate from different pools of progenitors. This is supported by the presence of α-SMA in the secondary bronchi at E11 (Tollet et al., 2001), even before *Fgf10*/β-galactosidase-positive cells are relocalized around the secondary bronchi (this report). However, from E13.5 onward, the smooth muscle cells around the secondary bronchi originate mostly from the *Fgf10*-expression domain, as indicated by the homogenous expression of β-galactosidase in the mesenchyme adjacent to the bronchial epithelium.

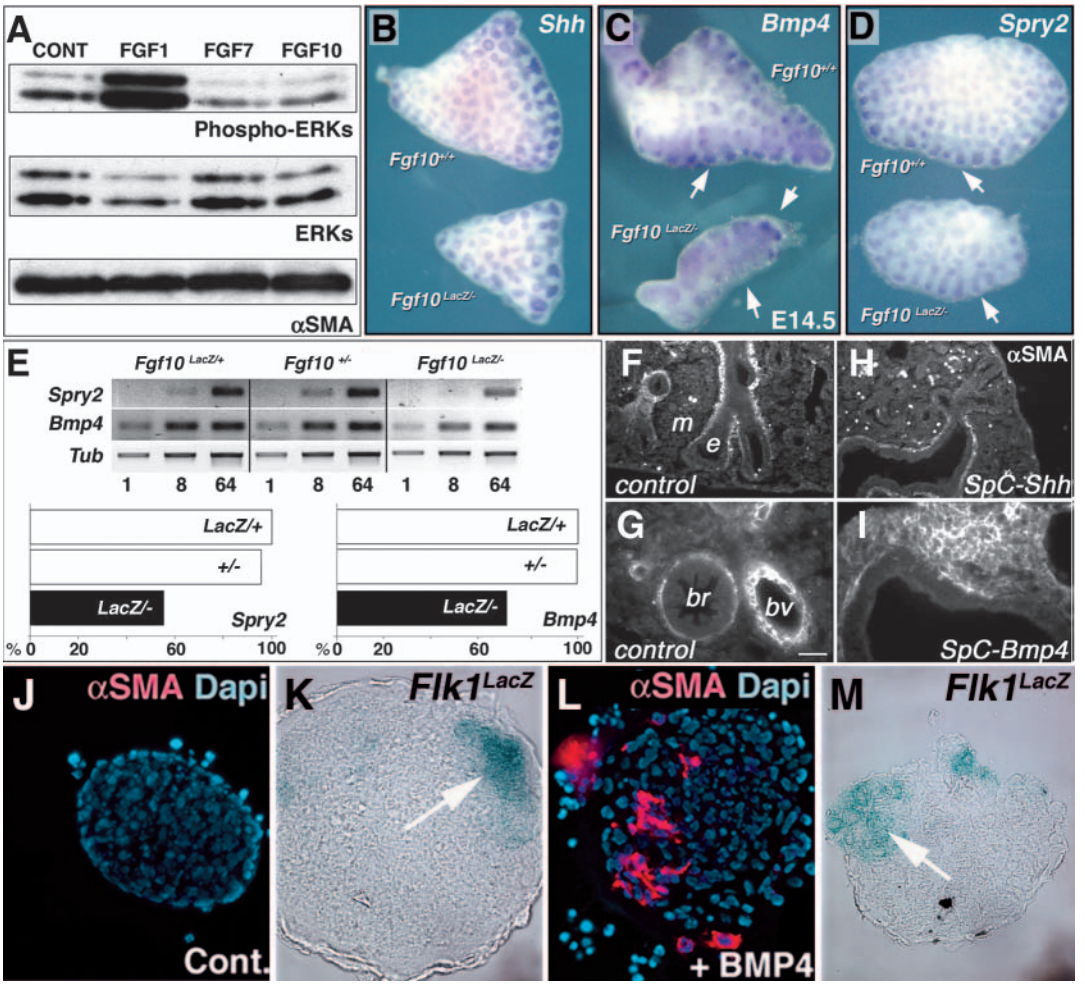

Fig. 5. FGF10 regulates the establishment of the parabronchial smooth muscle cell lineage via upregulation of *Bmp4* expression in the epithelium. (A) Treatment of lung SMC with either FGF1 or FGF7 or FGF10 (100 ng/ml) for 20 minutes. Only FGF1 induces the phosphorylation of 42/43 MAPK (upper bands). Total ERKs (after striping of the previous blot) and α-SMA blots correspond to loading controls. (B) Sonic hedgehog expression in E14.5 normal and $Fgf10^{LacZ/-}$ caudal lobes was used to outline the epithelial buds. Note that *Shh* expression is not significantly altered in the mutant lobe. (C) *Bmp4* expression in wild-type and $Fgf10^{LacZ/-}$ accessory lobes at E14.5, showing a lower expression level in the mutant lobe (white arrow). In the distal part, *Bmp4* expression level is less decreased. (D) *Sprouty2* expression in normal and mutant median lobes at E14.5, showing a lower expression level in the mutant lobe. (E) Semi-quantitative amplification course by PCR on gel electrophoresis. 1 (cycle 28), 8 (cycle 31) and 64 (cycle 34) amplification rate, respectively, showing decreased *Spry2 and Bmp4* mRNA level in $Fgf10^{LacZ/-}$ compared with $Fgf10^{LacZ/+}$ and $Fgf10^{+/-}$ lungs at E14.5. Quantification of *Spry2* and *Bmp4* expression by densitometry at 64 and 8 amplification rate, respectively. Ratios of *Spry2* to tubulin and *Bmp4* to tubulin in $Fgf10^{LacZ/+}$ lung are set to 100% and used as a reference. Note the decreased expression of *Sprouty2* and *Bmp4* in $Fgf10^{LacZ/-}$ lung compared to the reference (45% and 30% reduction, respectively). In both cases, *Spry2* and *Bmp4* expression levels were not decreased in $Fgf10^{+/-}$ lungs (respectively 95% and 99% of $Fgf10^{LacZ/+}$ expression level). (F-I) Comparison of α-SMA expression in wild-type, *SpC-Shh* and *SpC-Bmp4* transgenic lungs at E16.5. (F) Control lung showing α-SMA expression in the mesenchymal cells around the bronchial epithelium but excluded from the tip. (G) *SpC-Shh* lungs showing no disruption of α-SMA expression. (H) High magnification of a wild-type lung showing α-SMA expression around the bronchial epithelium and around the blood vessels. (I) α-SMA expression in *SpC-Bmp4* lungs showing a drastic increase of α-SMA expression in the distal mesenchyme. Note the expanded epithelium, which is characteristic of the *SpC-Bmp4* lungs. (J) Isolated E13.5 mesenchyme explants grown for 48 hours in Matrigel show no α-SMA-expressing cells by immunohistochemistry. (K) Identical experiment with mesenchyme explants from $Flk1^{LacZ/+}$ lungs to show the presence of endothelial cells in the explant (arrow). (L) Addition of recombinant 100 ng/ml of recombinant BMP4 induces α-SMA expression. (M) Identical experiment with $Flk1^{LacZ/+}$ mesenchymal explants shows the presence of endothelial cells within the BMP4-treated explant. Scale bar: 200 μm in B; 160 μm in C; 140 μm in D; 70 μm in F,G; 35 μm in H-K. br, bronchial epithelium; bv, blood vessels.

The distal location of this new subset of parabronchial SMC progenitors in the lung is reminiscent of the distal location of the progenitors for the various epithelial cell lineages of the lung (reviewed by Warburton et al., 2000). It is now of interest to determine whether the other mesenchymal lineages, including other types of SMCs (e.g. the vascular SMCs), lipocytes and endothelial cells, also originate in this domain. Interestingly, this domain of progenitor cells is also the area where budding morphogenesis is initiated (Bellusci et al., 1997b) and where many signaling molecules are expressed. This suggests that the distal lung buds act as signaling centers that synchronize morphogenetic events with differentiation.

FGF10 regulates the establishment of the parabronchial smooth muscle cell lineage via a non-autocrine effect on the lung bud epithelium

A difference in parabronchial SMC formation was observed in $Fgf10^{LacZ/-}$ lungs at all the stages investigated. The decreased β-galactosidase expression around the bronchial epithelium and the increased expression in the distal mesenchyme in $Fgf10^{LacZ/-}$ lungs strongly suggest that FGF10 regulates the entry of the SMC progenitors into the SMC program, rather than controlling the progenitor population. This is a new role for *Fgf10*, as to date its major role has seemed to be the regulation of budding and branching morphogenesis in a variety of organs (Min et al., 1998; Sekine et al., 1999) including the lung (Bellusci et al., 1997b). Interestingly, our in-vitro data indicate that the relocalization of the *Fgf10*-positive cells in the distal mesenchyme along the epithelium is essentially due to the growth of the distal epithelium into the distal mesenchyme. However, a comparison of Fig. 3D with Fig. 2E demonstrates that the domain of β-galactosidase-positive cells does not expand as proximally in vitro as it does in vivo, and that the branching pattern is disturbed. Therefore, we cannot exclude the fact that active migration of the mesenchyme does occur in vivo. It is therefore possible that the epithelium exerts a chemoattractive activity on cells derived from the distal mesenchyme, similar to the way the mesenchyme acts as a chemoattractant for the distal lung epithelium (Park et al., 1998).

Our cultures of primary lung mesenchyme in the presence of various recombinant FGFs demonstrated that FGF10, in contrast to FGF1, was not able to phosphorylate ERK and AKT. This indicates that FGF10 does not act in an autocrine fashion on the mesenchyme to fulfill its function in parabronchial SMC formation. At present, only FGF9 secreted by the mesothelium is implied in vivo in the biogenesis of parabronchial SMCs. It is proposed to signal through the mesenchymal receptor FGFR2c, and to maintain the mesenchymal progenitors in a proliferative and undifferentiated state (Weaver et al., 2003). By contrast, we propose that FGF10 uses an epithelial intermediate, BMP4.

Epithelial BMP4 is a candidate mediator of SMC formation

Our results indicate a decrease in *Bmp4* expression in $Fgf10^{LacZ/-}$ embryos. This reduction in *Bmp4* expression seems to primarily occur in the epithelium. These results are consistent with previous reports showing that FGF10 upregulates epithelial *Bmp4* transcription (Lebeche et al., 1999; Weaver et al., 2000). Overexpression of *Bmp4* in the distal lung epithelium using the surfactant protein C promoter led to ectopic expression of α-SMA in the distal mesenchyme. While addition of recombinant SHH induces α-SMA expression on isolated lung mesenchymal explants (Weaver et al., 2003), we show that overexpression of *Shh* in the distal lung epithelium in vivo does not modify α-SMA expression. This may be explained by the lack of upregulation of *Bmp4* in the epithelium or the mesenchyme upon overexpression of *Shh* in vivo (Bellusci et al., 1997a), by contrast to the induction of *Bmp4* expression by SHH in vitro (Weaver et al., 2003).

Consistent with a major role for *Bmp4* in SMC differentiation, recombinant BMP4 induced α-SMA expression in lung mesenchyme explants in vitro after 48 hours of culture. These results strongly suggest that BMP4 induces SMC formation by acting directly on the mesenchyme. We therefore propose that FGF10 expressed by the distal mesenchyme may contribute to parabronchial SMC formation via the upregulation of BMP4 synthesis by the epithelium. The failure to induce α-SMA expression in all cells can be explained by the presence of other cell types in the mesenchymal explants, e.g. the endothelial cells. In addition, these explants also contain a layer of mesothelium, producing FGF9, which has been shown to prevent the differentiation of the smooth muscle cells (Weaver et al., 2003).

Independent reports support the proposed role of BMP4 in smooth muscle cell differentiation. In the kidney, periureteral mesenchymal cells differentiate into smooth muscle cells at a site where *Bmp4* is highly expressed. In addition, E15.5 $Bmp4^{+/-}$ ureters have fewer α-SMA-positive cells (Miyazaki et al., 2003). Furthermore, in human lung fibroblast cultures, exogenous BMP4 inhibits proliferation and promotes smooth muscle cell differentiation, as indicated by increased expression of α-SMA and smooth muscle myosin (Jeffery et al., 2004).

The expression of the BMP antagonist noggin in parabronchial SMC (Weaver et al., 2003) suggests that regulation of BMP signaling may be important to finely tune SMC differentiation.

In conclusion, we demonstrate that the mesenchyme of the distal lung tip contains a set of progenitors for parabronchial SMCs that can be identified by *Fgf10*, and that normal transcription levels of at least one *Fgf10* allele are required for their entry into the parabronchial SMC lineage.

We are grateful to Drs Morgan Matthew, Klaus Kratochwil and Vesa Kaartinen for helpful comments on the manuscript, Daniel Meur and Dominique Morineau for the photographic reproductions, and Martine Blanche for skilled technical assistance in the mouse facility. We would also like to thank Dr Margaret Buckingham for making the *Mlc1v-nLacZ-24* line available to us. This work was supported by the Association pour la Recherche sur le Cancer (ARC) grant 5214, the Action Concertée Incitative 81/2001 – Biologie du Développement et Physiologie Intégrative, NIH RO1 HL074832-01 and HL75773-01 grants and the American Lung Association (CI-36-N) (S.B.). R.K. is an INSERM research fellow. A.M. received financial support from the French Ministry of Research and Technology as well as the ARC. J.V. received financial support from the European Commission (contract QLGA-CT-2000-51230), the CHLA Institutional award and the California Breast Cancer Research Program fellowship (10FB-0116).

References

Bellusci, S., Furuta, Y., Rush, M. G., Henderson, R., Winnier, G. and Hogan, B. L. (1997a). Involvement of Sonic hedgehog (Shh) in mouse embryonic lung growth and morphogenesis. *Development* **124**, 53-63.

Bellusci, S., Grindley, J., Emoto, H., Itoh, N. and Hogan, B. L. (1997b). Fibroblast growth factor 10 (FGF10) and branching morphogenesis in the embryonic mouse lung. *Development* **124**, 4867-4878.

Bellusci, S., Henderson, R., Winnier, G., Oikawa, T. and Hogan, B. L. (1996). Evidence from normal expression and targeted misexpression that bone morphogenetic protein (Bmp-4) plays a role in mouse embryonic lung morphogenesis. *Development* **122**, 1693-1702.

Hershenson, M. B., Naureckas, E. T. and Li, J. (1997). Mitogen-activated signaling in cultured airway smooth muscle cells. *Can. J. Physiol. Pharmacol.* **75**, 898-910.

Jeffery, T. K., Upton, P. D, Trembath, R. C. and Morrell, N. W. (2004). BMP4 inhibits proliferation and promotes myocyte differentiation of lung fibroblasts via Smad1 and JNK pathways. *Am. J. Physiol. Lung. Cell. Mol. Physiol.* **288**, L370-L378.

Kelly, R., Alonso, S., Tajbakhsh, S., Cossu, G. and Buckingham, M. (1995). Myosin light chain 3F regulatory sequences confer regionalized cardiac and skeletal muscle expression in transgenic mice. *J. Cell Biol.* **129**, 383-396.

Kelly, R. G., Brown, N. A. and Buckingham, M. E. (2001). The arterial pole of the mouse heart forms from Fgf10-expressing cells in pharyngeal mesoderm. *Dev. Cell* **1**, 435-440.

Lazaar, A. L. (2002). Airway smooth muscle: new targets for asthma pharmacotherapy. *Expert Opin. Ther. Targets* **6**, 447-459.

Lebeche, D., Malpel, S. and Cardoso, W. V. (1999). Fibroblast growth factor interactions in the developing lung. *Mech. Dev.* **86**, 125-136.

Lyons, G. E., Schiaffini, S., Sassoon, D., Barton, P. and Buckingham, M. (1990). Developmental regulation of myosin gene expression in mouse cardiac muscle. *J. Cell Biol.* **111**, 2427-2436.

Mailleux, A. A., Tefft, D., Ndiaye, D., Itoh, N., Thiery, J. P., Warburton, D. and Bellusci, S. (2001). Evidence that SPROUTY2 functions as an inhibitor of mouse embryonic lung growth and morphogenesis. *Mech. Dev.* **102**, 81-94.

Mailleux, A. A., Spencer-Dene, B., Dillon, C., Ndiaye, D., Savona-Baron, C., Itoh, N., Kato, S., Dickson, C., Thiery, J. P. and Bellusci, S. (2002). Role of FGF10/FGFR2b signaling during mammary gland development in the mouse embryo. *Development* **129**, 53-60.

Min, H., Danilenko, D. M., Scully, S. A., Bolon, B., Ring, B. D., Tarpley, J. E., DeRose, M. and Simonet, W. S. (1998). Fgf-10 is required for both limb and lung development and exhibits striking functional similarity to Drosophila branchless. *Genes Dev.* **12**, 3156-3161.

Miyazaki, Y., Oshima, K., Fogo, A. and Ichikawa, I. (2003). Evidence that bone morphogenetic protein 4 has multiple biological functions during kidney and urinary tract development. *Kidney Int.* **63**, 835-844.

Murase, S. and Horwitz, A. F. (2002). Deleted in colorectal carcinoma and differentially expressed integrins mediate the directional migration of neural precursors in the rostral migratory stream. *J. Neurosci.* **22**, 3568-3579.

Park, W. Y., Miranda, B., Lebeche, D., Hashimoto, G. and Cardoso, W. V. (1998). FGF-10 is a chemotactic factor for distal epithelial buds during lung development. *Dev. Biol.* **201**, 125-134.

Pepicelli, C. V., Lewis, P. M. and McMahon, A. P. (1998). Sonic hedgehog regulates branching morphogenesis in the mammalian lung. *Curr. Biol.* **8**, 1083-1086.

Raghu, G., Chen, Y. Y., Rusch, V. and Rabinovitch, P. S. (1998). Differential proliferation of fibroblasts cultured from normal and fibrotic human lungs. *Am. Rev. Respir. Dis.* **138**, 703-708.

Sekine, K., Ohuchi, H., Fujiwara, M., Yamasaki, M., Yoshizawa, T., Sato, T., Yagishita, N., Matsui, D., Koga, Y., Itoh, N. et al. (1999). Fgf10 is essential for limb and lung formation. *Nat. Genet.* **21**, 138-141.

Shalaby, F., Rossant, J., Yamaguchi, T. P., Gertsenstein, M., Wu, X. F., Breitman, M. L. and Schuh, A. C. (1995). Failure of blood-island formation and vasculogenesis in Flk-1-deficient mice. *Nature* **376**, 62-66.

Tollet, J., Everett, A. W. and Sparrow, M. P. (2001). Spatial and temporal distribution of nerves, ganglia, and smooth muscle during the early pseudoglandular stage of fetal mouse lung development. *Dev. Dyn.* **221**, 48-60.

Warburton, D., Schwarz, M., Tefft, D., Flores-Delgado, G., Anderson, K. D. and Cardoso, W. V. (2000). The molecular basis of lung morphogenesis. *Mech. Dev.* **92**, 55-81.

Weaver, M., Batts, L. and Hogan, B. L. (2003). Tissue interactions pattern the mesenchyme of the embryonic mouse lung. *Dev. Biol.* **258**, 169-184.

Weaver, M., Dunn, N. R. and Hogan, B. L. (2000). Bmp4 and Fgf10 play opposing roles during lung bud morphogenesis. *Development* **127**, 2695-2704.

Winnier, G., Blessing, M., Labosky, P. A. and Hogan, B. L. (1995). Bone morphogenetic protein-4 is required for mesoderm formation and patterning in the mouse. *Genes Dev.* **9**, 2105-2116.

Yang, Y., Palmer, K. C., Relan, N., Diglio, C. and Schuger, L. (1998). Role of laminin polymerization at the epithelial mesenchymal interface in bronchial myogenesis. *Development* **125**, 2621-2629.

Yang, Y., Relan, N. K., Przywara, D. A. and Schuger, L. (1999). Embryonic mesenchymal cells share the potential for smooth muscle differentiation: myogenesis is controlled by the cell's shape. *Development* **126**, 3027-3033.

Yao, H. H., Whoriskey, W. and Capel, B. (2002). Desert Hedgehog/Patched 1 signaling specifies fetal Leydig cell fate in testis organogenesis. *Genes Dev.* **16**, 1433-1440.

Zhang, J., O'Shea, S., Liu, J. and Schuger, L. (1999). Bronchial smooth muscle hypoplasia in mouse embryonic lungs exposed to a laminin beta1 chain antisense oligonucleotide. *Mech. Dev.* **89**, 15-23.